

## Recombination and Ion-Conversion Processes of Argon Ions\*

G. E. Veatch and H. J. Oskam

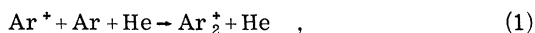
*Department of Electrical Engineering, University of Minnesota, Minneapolis, Minnesota 55455*

(Received 8 December 1969)

The properties of  $\text{Ar}^+$  and  $\text{Ar}_2^+$  were studied in helium-argon mixtures by means of the afterglow method. The time dependence of the number density of these ions was measured by mass-spectrometric techniques. The temporal behavior of the intensity of various spectral lines was also determined. The studies established the occurrence of the collisional recombination process  $\text{Ar}^+ + 2e \rightarrow \text{Ar} + e + h\nu$ , while they confirmed the importance of the dissociative recombination process  $\text{Ar}_2^+ + e \rightarrow \text{Ar} + \text{Ar} + h\nu$ . The collisional process appeared to populate all levels studied, while the dissociative process selectively populated the  $2p$  and  $3p$  energy levels. The only ion-molecule-association reaction observed for argon concentrations between 0.01 and 5% was  $\text{Ar}^+ + \text{Ar} + \text{He} \rightarrow \text{Ar}_2^+ + \text{He}$ . The rate constant was found to be  $8.0 \times 10^{-32} \text{ cm}^6 \text{ sec}^{-1}$ . The value of the mobility of  $\text{Ar}^+$  in the helium-argon mixtures obeyed Blanc's Law.

### I. INTRODUCTION

The first studies of the properties of decaying plasmas produced in helium-argon mixtures were reported by Biondi.<sup>1</sup> He measured the time dependence of the electron density by means of the microwave cavity technique and obtained a value for the mobility of the  $\text{Ar}^+$  ions in helium, i. e.,  $\mu_0(\text{Ar}^+) = 21 \text{ cm}^2/\text{V sec}$ . The comparisons of these studies with those performed in pure argon showed that the large electron-ion recombination coefficient measured in decaying argon plasmas was related to the  $\text{Ar}_2^+$  ions. The only other study of decaying plasmas in helium-argon mixtures was reported in 1958 by Oskam<sup>2</sup> using the same measuring technique. The value of  $\mu_0(\text{Ar}^+)$  was in very good agreement with Biondi's value, while the studies also established the occurrence of the ion-molecule association reaction



with a rate coefficient of  $8.5 \times 10^{-32} \text{ cm}^6/\text{sec}$ .

The main purpose of the studies reported in the present paper was to obtain the relationship between the time dependence of the ion densities and that of the intensity of various spectral lines during the decay period of plasmas produced in helium-argon mixtures. These studies give information about the electron-ion recombination processes involving  $\text{Ar}^+$  and  $\text{Ar}_2^+$  ions.

A study of the relation between light emission and the recombination process for  $\text{Ar}_2^+$  was reported by Redfield and Holt.<sup>3</sup> They performed electron-density and light-emission measurements during the decay period of argon plasmas. The authors were unable to determine the origin of the

light emission during the afterglow period. Recently however, Frommhold and Biondi<sup>4</sup> showed that certain spectral lines emitted during the argon afterglow originate at least in part from the dissociative recombination of  $\text{Ar}_2^+$  with electrons. They studied the shape of spectral lines and observed an increased width of the line during the plasma decay period with an evident shoulder structure present. This type of line profile is to be expected as a result of emission from a level populated by the dissociative recombination process.

The recombination process involving  $\text{Ar}^+$  has not been studied previously and no information about the spectral distribution of the emission due to this process has been reported. Moreover, the present study is the first mass-spectrometric investigation of decaying plasmas produced in helium-argon mixtures.

### II. EXPERIMENTAL METHOD

The experimental tube used to study the time dependence of the ions during the afterglow period consists of a differentially pumped mass spectrometer which samples ions diffusing to the walls of a discharge tube. The mass spectrometer used is of the electric quadrupole type and has been described in detail elsewhere.<sup>5</sup>

The discharge region is a glass cylinder with metal end plates. One end plate is a molybdenum electrode, while the other is made of kovar metal and contains a small hole (60- $\mu$  diam and 40- $\mu$  length) through which the ions effuse into the mass-spectrometer region.

The gas handling system is analogous to that developed by Alpert.<sup>6</sup> The ultimate pressure was about  $10^{-9}$  Torr following a system bakeout at

350 °C for a period of 24–36 h. All research-grade pure gases admitted to the discharge region were purified by means of the cataphoretic segregation method.<sup>7</sup> For the studies of plasmas produced in gas mixtures, each gas was separately cataphoretically purified before mixing. The final cleaning of the discharge region was achieved by covering the discharge-tube wall with a molybdenum layer obtained from sputtering the discharge electrode. This cleaning process was continued until the impurity-ion signal was less than 0.5% of that of the dominant ion. This condition was necessary to achieve reproducibility of the data. The gas pressure was measured by a capacitance manometer which controlled a servo-operated valve to maintain a constant preset pressure in the discharge tube.

A block diagram of the measuring system is shown in Fig. 1. The discharge was produced by a high-voltage dc pulse applied between the discharge-tube electrodes. The ions passing through the quadrupole mass spectrometer are detected by a 14-stage ion multiplier. The resulting anode pulses, each due to a single ion, are amplified by a wideband amplifier and those above a minimum pulse height are selected by a discriminator in order to reduce the background count rate. The pulses from the discriminator are then fed into a multichannel scaler. The afterglow is divided into 100 to 400 equal-time intervals which have a minimum duration of 25  $\mu$ sec. As the multichannel scaler advances from channel to channel, the num-

ber of pulses in the corresponding time intervals in the afterglow are recorded in the memory section. By accumulating the afterglow counts for a sufficient number of afterglow repetitions, a statistically significant number of counts can be recorded in each channel of the memory.

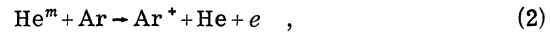
The time dependence of the intensity of the spectral lines studied was obtained using a 0.5-m Ebert light spectrometer. The photomultiplier had a S-20 photocathode and was cooled to reduce the dark-count rate. The signal pulses resulting from single photons were detected and counted using the same technique used for ions.

### III. RELEVANT AFTERGLOW PROCESSES AND THEORY

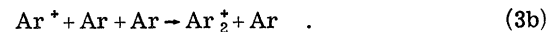
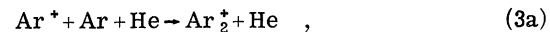
The equations which describe the behavior of the plasma constituents during the decay period will be given only if they are pertinent to the particular case under investigation. In the discussion that follows it will be assumed that sufficient time has elapsed after the cessation of the discharge excitation to ensure that all plasma constituents are in thermal equilibrium with each other.

#### A. Ion-Density Time Dependence

The experimental conditions were chosen such that during the plasma decay period the only ions present were  $\text{Ar}^+$  and  $\text{Ar}_2^+$ . The  $\text{Ar}^+$  ions are produced in the afterglow by the Penning ionization process



where  $\text{He}^m$  is a metastable helium atom. The  $\text{Ar}_2^+$  ions are produced in the afterglow by conversion of  $\text{Ar}^+$  into  $\text{Ar}_2^+$  by the following reactions:



The equations which describe the rate of change of the densities of  $\text{Ar}^+$ ,  $\text{Ar}_2^+$ , and  $\text{He}^m$  during the decay period, neglecting the influence of ionization processes due to mutual collisions between metastable atoms, are

$$\frac{\partial M(\vec{r}, t)}{\partial t} = D_m \nabla^2 M(\vec{r}, t) - \nu_d M(\vec{r}, t) \quad , \quad (4)$$

$$\begin{aligned} \frac{\partial n_1(\vec{r}, t)}{\partial t} = & D_{a_1} \nabla^2 n_1(\vec{r}, t) - \nu_a n_1(\vec{r}, t) \\ & - \alpha_1 n_1(\vec{r}, t) n_e(\vec{r}, t) + \nu_d M(\vec{r}, t) \quad , \quad (5) \end{aligned}$$

$$\begin{aligned} \frac{\partial n_2(\vec{r}, t)}{\partial t} = & D_{a_2} \nabla^2 n_2(\vec{r}, t) \\ & - \alpha_2 n_2(\vec{r}, t) n_e(\vec{r}, t) + \nu_a n_1(\vec{r}, t) \quad . \quad (6) \end{aligned}$$

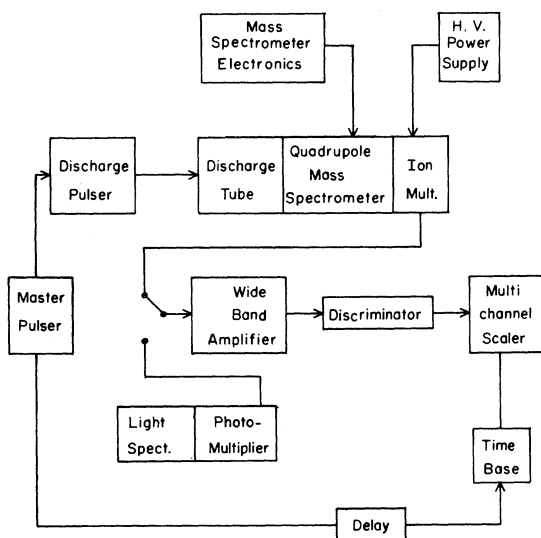


FIG. 1. Block diagram of measuring system.

Here,  $M$ ,  $n_1$ ,  $n_2$ , and  $n_e$  are the densities of the metastable atoms,  $\text{Ar}^*$ ,  $\text{Ar}_2^*$ , and electrons, respectively;  $D_a$  is the ambipolar diffusion coefficient;  $D_m$  is the metastable particle diffusion coefficient;  $\nu_c$  is the conversion frequency due to processes (3);  $\nu_d$  is the destruction frequency of metastable particles due to process (2);  $\alpha$  is the recombination coefficient.

If the loss of the atomic ions by recombination is negligible compared to that by diffusion and conversion, Eqs. (4) and (5) can be solved for the boundary condition of zero density at the walls of the plasma container. The time-dependent part of the fundamental diffusion-mode solution is

$$M(0, t) = M(0, 0)e^{-t/\tau_m} \quad , \quad (7)$$

$$n_1(0, t) = [n_1(0, 0) - A]e^{-t/\tau_1} + Ae^{-t/\tau_m} \quad , \quad (8)$$

$$\text{with } 1/\tau_m = D_m/\Lambda^2 + \nu_d \quad , \quad (9)$$

$$1/\tau_1 = D_{a1}/\Lambda^2 + \nu_c \quad , \quad (10)$$

$$\text{and } A = \frac{\nu_d}{1/\tau_1 - 1/\tau_m} \quad . \quad (11)$$

Here,  $\Lambda$  is the characteristic diffusion length of the container corresponding to the fundamental-mode solution.

Equation (6) cannot be solved analytically for the present experimental conditions since in general neither the diffusion loss nor the recombination loss of the molecular ions can be neglected with respect to each other. The previous equations, however, are sufficient for explaining the measured time dependences of the ion densities.

An effect which must be taken into account in helium-argon mixtures is the change in the value of the ion mobility as a function of the concentration of argon in helium. This effect appears at relatively low argon concentrations since the mobility of  $\text{Ar}^*$  in argon is very different from the mobility of  $\text{Ar}^*$  in helium. The value of the mobility  $\mu$  is believed to obey Blanc's Law, i. e.,

$$1/\mu = f_a/\mu_a + (1 - f_a)/\mu_b \quad , \quad (12)$$

where  $f_a$  is the fractional concentration of gas  $a$  in gas  $b$ . The mobilities  $\mu_a$  and  $\mu_b$  are the "pure gas" mobilities for the  $\text{Ar}^*$  ion in each of the gases. The theoretical justification for this expression is due to Holstein<sup>8</sup> and has been discussed by Biondi and Chanin.<sup>9</sup>

#### B. Time Dependence of the Light Emission Intensity

The argon atomic light emission in the afterglow can result from recombination of the atomic ion,  $\text{Ar}^*$ , and/or from dissociative recombination of the molecular argon ion  $\text{Ar}_2^*$ . Fortunately, the present studies show that the dissociative recombination of

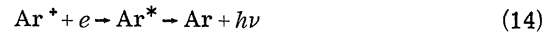
$\text{Ar}_2^*$  does not populate all energy levels of the neutral atom, so that it was possible to differentiate between the emission due to recombination of  $\text{Ar}^*$  and that due to recombination of  $\text{Ar}_2^*$ .

A few possible recombination processes involving the atomic argon ion will first be discussed. The time-dependent part of the light intensity  $I_a(t)$  will be proportional to the product of the recombination coefficient, the ion density, and the electron density, i. e.,

$$I_a(t) \propto \alpha_1 n_1(t) n_e(t) \quad . \quad (13)$$

If the time dependences of  $I_a(t)$ ,  $n_e(t)$ , and  $n_1(t)$  each can be described by an exponential function with time constants  $\tau_a$ ,  $\tau_e$ , and  $\tau_1$ , respectively, then the various time constants may be compared in order to determine what type of recombination process is responsible for the light emission. The exponential time dependences can be achieved by choosing the experimental conditions such that the loss of particles is determined by linear processes, i. e., the recombination loss is small compared to loss by diffusion and conversion into another particle.

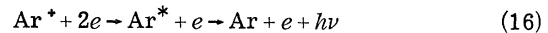
The radiative recombination process



will result in atomic light emission with a time constant given by

$$1/\tau_a = 1/\tau_1 + 1/\tau_e \quad . \quad (15)$$

The collisional recombination process

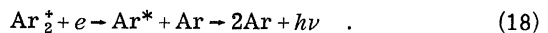


will result in a time constant of the atomic light emission given by

$$1/\tau_a = 1/\tau_1 + 2/\tau_e \quad , \quad (17)$$

provided the emission originates from electronic transitions between energy levels with sufficiently small principal quantum numbers and provided the recombination coefficient is proportional to the electron density. Previously, it was established that the recombination process involving  $\text{He}^*$  or  $\text{Ne}^*$  was a collisional recombination process with a recombination coefficient proportional to the electron density.<sup>10-12</sup>

The recombination process involving  $\text{Ar}_2^*$  has been established by line-profile studies<sup>4</sup> and inferred from the large recombination rate to be the dissociative recombination process<sup>1,3</sup>



The time constant for the intensity of the light emitted due to process (18) is given by

$$1/\tau_a = 1/\tau_e + 1/\tau_2 \quad . \quad (19)$$

It is rather doubtful, however, whether the  $\text{Ar}_2^+$  decay is ever exponential. Thus, the only way to determine whether or not the light emission is due to process (18) is to compare the product of the electron density and the  $\text{Ar}_2^+$  density with the light-emission intensity involved. This method constitutes a more general method of comparing the light-intensity time dependence with that of the charged particles involved in the recombination process.

#### IV. RESULTS AND DISCUSSION

The discussion of the experimental results will be divided into two parts. The first part relates to studies on helium containing 0.1 and 0.01% argon. Under this condition,  $\text{Ar}^+$  was the only ion detected in the afterglow. No  $\text{Ar}_2^+$  was observed since the conversion of  $\text{Ar}^+$  into  $\text{Ar}_2^+$  was very small. The second part relates to argon concentrations of 1 and 5%. For these mixtures, both  $\text{Ar}^+$  and  $\text{Ar}_2^+$  could be detected in the afterglow, although the  $\text{Ar}_2^+$  density was small compared to that of  $\text{Ar}^+$ . Thus, the time dependence of the electron density was known in both situations, i. e., equal to that of the  $\text{Ar}^+$  ions.

##### A. Small Argon Concentrations (0.01 and 0.1%)

For these concentrations,  $\text{Ar}^+$  was the only ion detected in the afterglow and the time dependence of the density was exponential with a  $p_0/\tau_1$  value independent of pressure ( $p_0$  is the total reduced gas pressure). Therefore, the ion disappeared from the plasma by ambipolar diffusion to the walls of the discharge container. The cross section for process (2) is sufficiently large<sup>13</sup> to ensure that, under the present conditions,  $\text{He}^m$  is destroyed during the very early afterglow. Therefore, the influence of the production of  $\text{Ar}^+$  by helium metastable atoms on the decay of  $\text{Ar}^+$  can be neglected. The ambipolar diffusion coefficient obtained for the atomic argon ion in helium is  $D_{a1}p_0 = 770 \text{ cm}^2 \text{ sec}^{-1} \text{ Torr}$  at a gas temperature of 300 °K. This corresponds to a mobility of  $19.5 \text{ cm}^2 (\text{V sec})^{-1}$  for  $\text{Ar}^+$  in "pure helium," since corrections due to Blanc's Law are negligible for these low argon concentrations.

The light intensity decay for various atomic-argon lines was measured as a function of time in the afterglow. These measurements were performed for conditions under which only the  $\text{Ar}^+$  ion could be observed mass spectrometrically. All the spectral lines observed during the decay period had the same decay rate which became exponential during the later part of the afterglow. The functional relationship between the density of  $\text{Ar}^+$  and the intensity of the atomic light emission was determined by eliminating the time parameter. The

light intensity at various times during the decay period was plotted versus the  $\text{Ar}^+$  ion density at the same times for identical experimental conditions. One of the results of this procedure is shown in curve (a) of Fig. 2.

The relation between the time constants is very nearly given by

$$1/\tau_a = 3/\tau_1 \quad (20)$$

This is the same relation as given by Eq. (17) since the electron density is equal to the  $\text{Ar}^+$  ion density. Many other light and ion-density curves were analyzed in the same manner and yielded the same result. Therefore, the recombination process involving the atomic argon ion is, for the present experimental conditions, the collisional recombination process (16) with a recombination coefficient proportional to the electron density.<sup>14</sup> This process appears to populate directly or indirectly all atomic levels from which transitions were observed in the 3000–7000 Å range.

##### B. Argon Concentrations of 1 and 5%

For these concentrations, the  $\text{Ar}_2^+$  ion was detected during the plasma decay period. It was also found that  $p_0/\tau_1$  for  $\text{Ar}^+$  was not independent of pressure. This is due to the influence of the conversion process (3a) on the decay rate of  $\text{Ar}^+$ . The influence of reaction (3b) will be negligible for the concentrations considered here. The results of these measurements of the  $\text{Ar}^+$  decay time con-

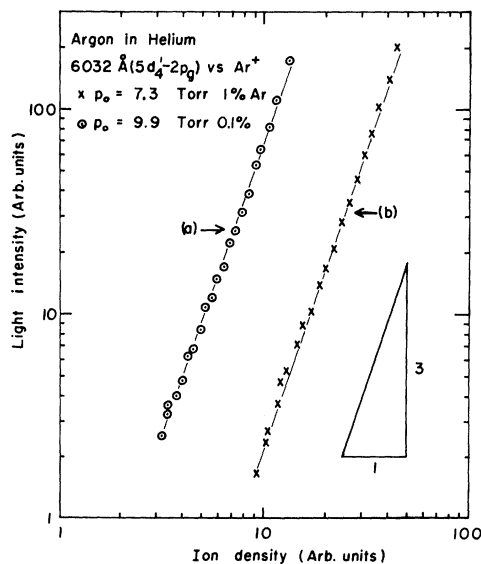


FIG. 2. Intensity of the 6032 Å line of argon versus the  $\text{Ar}^+$  ion density during the decay period. Each data point corresponds to the values of the ion density and light intensity at a given time in the afterglow.

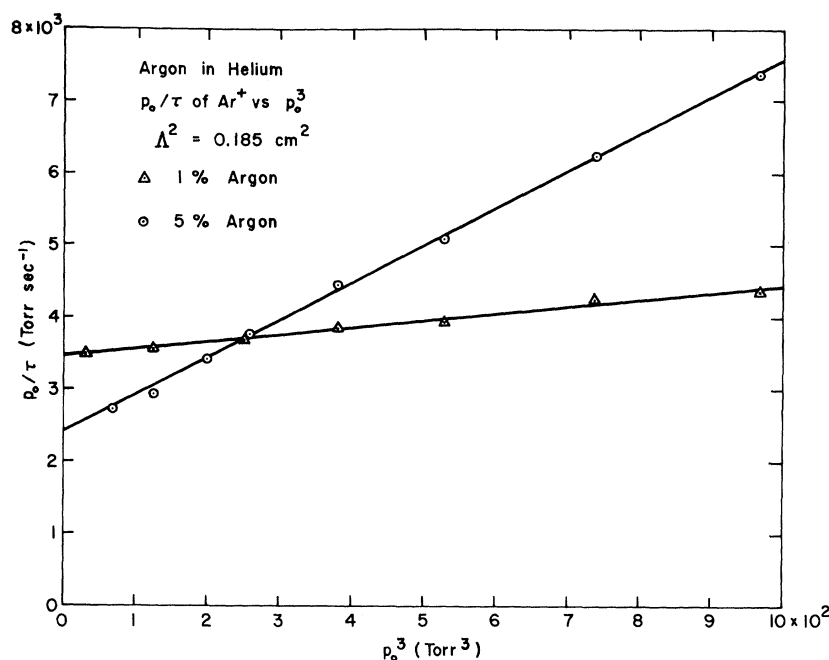


FIG. 3. Measured values of  $p_0/\tau$  for  $\text{Ar}^+$  as a function of  $p_0^3$  for two argon concentrations at a gas temperature of 300°K. ( $p_0$  is the total reduced gas pressure.)

stant as a function of  $p_0^3$  are shown in Fig. 3 for argon concentrations of 1 and 5%. Since the  $p_0/\tau_1$  values are a linear function of  $p_0^3$  a three-body process is obviously involved. Both argon concentrations yielded the same value for the conversion frequency if the conversion frequency was assumed to be a linear function of argon concentration as is the case for process (3a). The value of the conversion frequency measured is  $\nu_c = 100 p_0(\text{Ar}) p_0(\text{He}) \text{ sec}^{-1}$  at a gas temperature of 300°K. The corresponding rate constant is  $k = 8.0 \times 10^{-32} \text{ cm}^6 \text{ sec}^{-1}$ . This value for reaction (3a) is in excellent agreement with the value obtained by Oskam but somewhat lower than the value estimated by the ESSA group.<sup>15</sup>

Neither of the straight lines shown in Fig. 3 extrapolates at zero pressure to the "pure-helium" mobility value for  $\text{Ar}^+$ , which would correspond to a value of  $p_0/\tau_1$  of  $4.15 \times 10^3 \text{ Torr sec}^{-1}$ . This is due to the influence of argon atoms on the mobility of  $\text{Ar}^+$  in the mixture.

The mobility values obtained from the extrapolation of the  $p_0/\tau_1$  lines to zero pressure should obey Blanc's law. The inverse of the measured mobility values are plotted as a function of argon concentration in Fig. 4. The straight line is calculated using Blanc's law, where  $\mu_0(\text{Ar}^+ \text{ in He}) = 19.5 \text{ cm}^2(\text{V sec})^{-1}$  and  $\mu_0(\text{Ar}^+ \text{ in Ar}) = 1.4 \text{ cm}^2 \times (\text{V sec})^{-1}$  are used. The pure-argon mobility used is that obtained in ion-drift-tube measurements.<sup>16</sup> The measured values agree very well with the calculated dependence of the mobility on argon concentration.

Observation of the light intensity when both  $\text{Ar}^+$  and  $\text{Ar}_2^+$  ions are present allows for the correlation of any changes in the decay rates of the intensity of afterglow line emissions with the appearance of the  $\text{Ar}_2^+$  ion. This should reveal the type of recombination process related to  $\text{Ar}_2^+$  ions.

The result of the comparison is that when  $\text{Ar}_2^+$  ions are present spectral lines originating from the  $2p$  and  $3p$  levels of the argon atom decayed at a slower rate than the other levels.<sup>17</sup> The other energy levels are apparently still populated solely by the collisional recombination process involving the  $\text{Ar}^+$  ion. Curve (b) in Fig. 2 is typical of levels for which the population density did not change its time dependence.

The low-argon-concentration studies showed that the  $2p$  and  $3p$  levels are also populated by the collisional recombination of  $\text{Ar}^+$  with electrons. Therefore, it is reasonable to assume that the change in the decay properties of the intensities of lines originating from the  $2p$  and  $3p$  levels for larger argon concentrations is due to an additional population process of these levels due to the recombination of  $\text{Ar}_2^+$  with electrons. Curves (a) and (d) of Fig. 5 show the time dependence of the intensities of the 6965 Å ( $2p \rightarrow 1s_5$ ) and 6032 Å ( $5d_4 \rightarrow 2p_9$ ) spectral lines. The decay properties of these two lines are clearly quite different, especially during the later part of the decay period.

If the dissociative recombination of  $\text{Ar}_2^+$  with electrons contributes significantly to the population of the  $2p$  and  $3p$  levels the time dependence of the intensity of lines originating from these levels

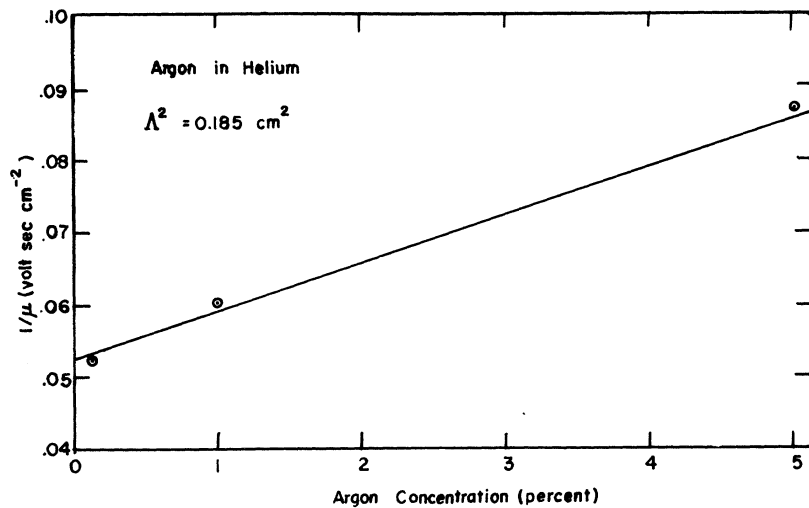


FIG. 4. Measured values for the inverse of the  $\text{Ar}^+$  mobility  $\mu$  in helium-argon mixtures as a function of argon concentration.

should be the same as that of the product of the  $\text{Ar}_2^+$  ion density and the electron density. Curve (b) in Fig. 5 shows the time dependence of the product of the  $\text{Ar}_2^+$  and  $\text{Ar}^+$  ion densities. (The  $\text{Ar}^+$  density was equal to the electron density.) Curves

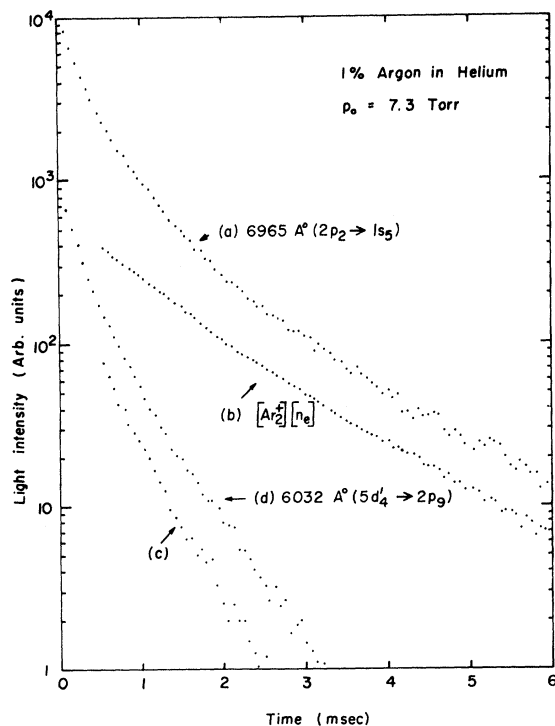


FIG. 5. Time dependence in the afterglow of: (a) the 6965 Å ( $2p_2 \rightarrow 1s_5$ ) line; (b) the product of the  $\text{Ar}_2^+$  density and the electron density, which was equal to the  $\text{Ar}^+$  density; (c) the difference between curves (a) and (b) after the two have been normalized in the late afterglow; (d) the 6032 Å ( $5d_4 \rightarrow 2p_9$ ) line.

(a) and (b) show clearly the same time dependence during the later part of the afterglow period, which proves that during this period the emission of the 6965 Å line is due to the dissociative recombination of  $\text{Ar}_2^+$  with electrons. It thus appears that the dissociative recombination process selectively populates the argon energy levels. The  $2p$  and  $3p$  levels are most probably populated directly, while lower-lying levels can be populated indirectly by cascading.

The time dependences of curves (a) and (b) in Fig. 5 differ appreciably during the early afterglow period. Curve (c) is obtained from curves (a) and (b) by subtraction after curves (a) and (b) are made to coincide during the late-afterglow period. No differences smaller than ten percent of the emission signal were used. Curve (c) has been shifted downwards for comparison with curve (d), which is the time dependence of the intensity of a spectral line which resulted solely from the collisional recombination of  $\text{Ar}^+$  ions with electrons. The close agreement in the time dependence of curves (c) and (d) shows that a significant part of the 6965 Å line emission during the early afterglow period is due to the atomic-ion-recombination process.

## V. CONCLUSIONS

The studies presented relate to the simultaneous measurement of the time dependences of the number density of  $\text{Ar}^+$  and  $\text{Ar}_2^+$  ions and that of the intensity of spectral lines during the decay period of plasmas produced in helium-argon mixtures.

For argon concentration of 0.01 and 0.1%, only  $\text{Ar}^+$  ions were detected and collisional recombination of these ions with electrons was found to be the origin of the spectral line emission in the spectral range (3000–7000 Å) studied. All the atomic energy levels studied were populated by

the collisional recombination process of  $\text{Ar}^+$ . The same results were obtained previously for the helium and neon atomic ions.<sup>10-12</sup>

For argon concentrations of 1 and 5%,  $\text{Ar}_2^+$  ions were also observed, although, for the experimental conditions, the  $\text{Ar}^+$  ions were the majority ions. These studies led to the verification, for the first time by simultaneous light emission and ion-density measurements, of the dissociative recombination of  $\text{Ar}_2^+$  with electrons. The importance of this recombination process has previously been estab-

lished by line-broadening studies<sup>4</sup> as well as by the large recombination coefficient measured for the  $\text{Ar}_2^+$  ion.<sup>1,3</sup> The present studies strongly indicate that the dissociative recombination process populates directly only the  $2p$  and  $3p$  energy levels.

#### ACKNOWLEDGMENT

The discussions with other members of the study group on collision processes have been very helpful.

\*Work supported by the Air Force Research Laboratories, Office of Aerospace Research (Contract No. AF 19(628)-4794) and National Science Foundation (Grant No. GK-10395).

<sup>1</sup>M. A. Biondi, *Phys. Rev.* **83**, 1078 (1951).

<sup>2</sup>H. J. Oskam, *Philips Res. Rept.* **13**, 335 (1958).

<sup>3</sup>A. Redfield and R. B. Holt, *Phys. Rev.* **82**, 874 (1951).

<sup>4</sup>L. Frommhold and M. A. Biondi, *Phys. Rev.* **185**, 244 (1969).

<sup>5</sup>G. F. Sauter, R. A. Gerber, and H. J. Oskam, *Rev. Sci. Instr.* **37**, 572 (1966).

<sup>6</sup>D. Alpert, *J. Appl. Phys.* **24**, 860 (1953).

<sup>7</sup>R. Riesz and G. H. Dieke, *J. Appl. Phys.* **25**, 196 (1954).

<sup>8</sup>T. Holstein, *Phys. Rev.* **100**, 1230 (1955).

<sup>9</sup>M. A. Biondi and L. M. Chanin, *Phys. Rev.* **122**, 843 (1961).

<sup>10</sup>R. A. Gerber, G. F. Sauter, and H. J. Oskam, *Physica* **32**, 2173 (1966).

<sup>11</sup>G. F. Sauter, R. A. Gerber, and H. J. Oskam, *Physica* **32**, 1921 (1966).

<sup>12</sup>G. E. Veatch and H. J. Oskam (unpublished).

<sup>13</sup>A. V. Phelps, *Proceedings of the Third International Conference on Ionization Phenomena in Gases, Venice, 1957* (unpublished), p. 818.

<sup>14</sup>Principal quantum number of the energy levels studied is believed to be sufficiently small such that the emission intensity is proportional to the recombination rate.

<sup>15</sup>D. K. Bohme, D. B. Dunkin, F. C. Fehsenfeld, and E. E. Ferguson, *J. Chem. Phys.* **51**, 863 (1969).

<sup>16</sup>K. B. McAfee, D. Sipler, and D. Edelson, *Phys. Rev.* **160**, 160 (1967).

<sup>17</sup>Paschen notation is used for the levels.

## Excitation of Ionized Helium States in a Cooled Hollow-Cathode Discharge\*

H. G. Berry<sup>†</sup> and F. L. Roesler

*Department of Physics, University of Wisconsin, Madison, Wisconsin 53706*

(Received 3 April 1969; revised manuscript received 26 November 1969)

A high-resolution study of the  $\text{He II } \lambda 4686 \text{ \AA}$  ( $n=3-4$ ) line complex emitted from a cooled hollow cathode has been made using a double-etalon spectrometer with photoelectric detection. Computer analysis of the digitally recorded spectra of this line yields fine-structure and isotope-shift measurements for the isotopes  $^3\text{He}$  and  $^4\text{He}$  which agree with quantum electrodynamic theory to within  $\pm 0.0005 \text{ cm}^{-1}$  for the best measured components. The excitation and deexcitation processes for this transition, which are active in the hollow-cathode, have been analyzed. The results show that the anomalously large widths observed in ionized helium lines which have been electronically excited arise from large momentum transfers in the excitation process. Calculation of the momentum-transfer line profile in the process  $\text{He} + e \rightarrow \text{He}^{+*} + e + e$  gives reasonable agreement with the observed profiles when the instrumental profile and neutral He Doppler profile are included. Measurements further confirm that the origin of the small anode-drift shift is a residual electric field within the discharge.